Computer Simulation of Oxygen Tension Histograms – A Possibility for Interpretation of Microelectrode Measurements[1]

Oxygen microelectrode measurements can be performed in the microstructure of the tissue and oxygen tension distribution is measured directly at the capillary and cellular level. Most of the microelectrode results are illustrated in form of oxygen tension frequency distributions (histograms). Some hundreds of oxygen tension values are measured in a small tissue volume and frequency of the oxygen tension values is illustrated as a function of local oxygen tension value (KUNZE[2], LÜBBERS[3], WHALEN and NAIR[4]).

Question arises as to what extent the oxygen tension histogram is dependent on the capillary arrangement. Are differences to be found in oxygen tension histograms of capillary systems with homogeneous and inhomogeneous microcirculation? How is the oxygen tension histogram distributed under hypoxic conditions? Answers to part of these questions are given on the basis of oxygen tension histograms of homogeneously perfused con- and countercurrent as well as inhomogeneously perfused capillary network systems. To obtain an overall impression on the importance and validity of oxygen tension histograms, a digital computer simulation is performed based on Fick's first law and the partial differential equation of diffusion.

Method. The method of calculation is based on a set of assumptions which are necessary for model construction and derivation of differential equations for capillaries and tissue. The assumptions are similar to those originally used by KROGH[5].

a) The tissue consists of a quadratic network with 3×3 quadratic capillary meshes. The total tissue area has 2 inputs and 2 outputs (arterioles and venules) (Figure 1). In the case of con- and countercurrent systems the same number of capillaries per unit of tissue volume and the same blood flow were used in the examination. b) The oxygen consumption is homogeneous and corresponds to that of a cube with the side length of the capillary mesh system. c) The capillary network as well as con- and countercurrent systems are symmetric and continue in the same way to infinity. Arterioles and venules are evenly distributed in the whole tissue. d) The oxygen consumption rate is assumed according to the Law of Michaelis and Menten. e) Capillary cross-section is quadratic. f) Within the capillaries diffusion- and convec-

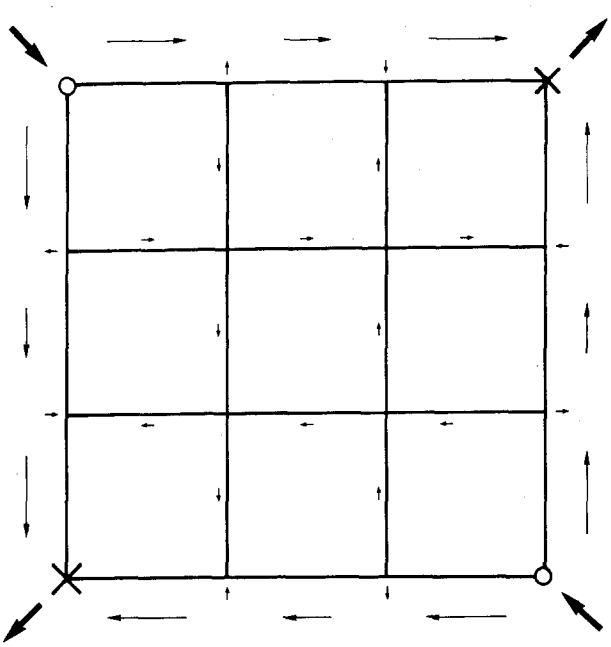

Fig. 1. Capillary network systems in brain tissue with 3×3 quadratic capillary meshes and 2 arterioles and 2 venules (arrows = input and output of blood flow). The length of the arrows reflects differences in blood flow rate in the various capillaries.

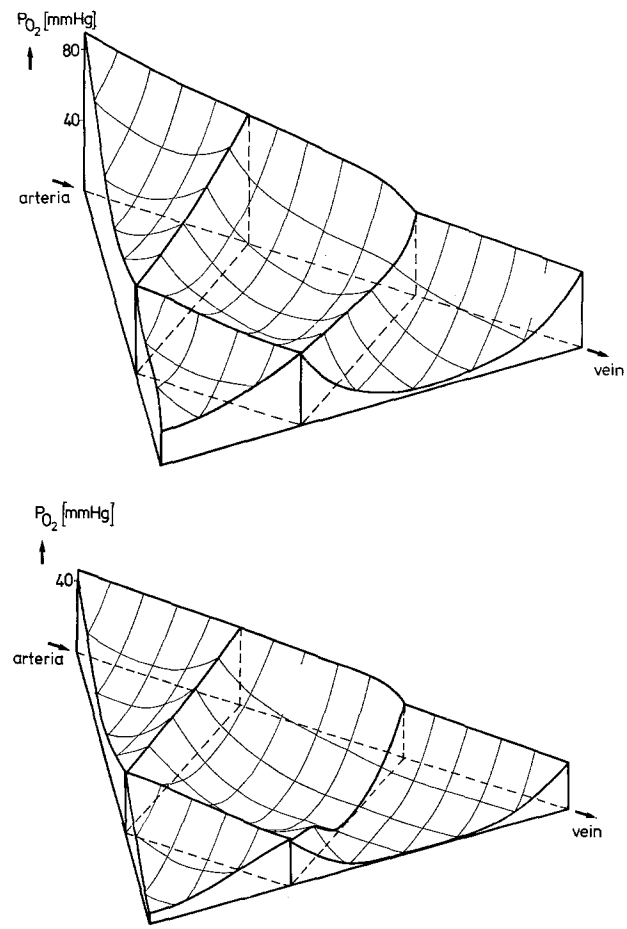

Fig. 2. Oxygen tension (P_{O_2}) distribution in brain tissue during normoxia. For reasons of symmetry only $^1/_4$ of the whole network can be seen. Dotted lines mark the capillaries. Upper part: Normal oxygen supply of the tissue. Input parameters of the computer program: $AG = 4.28$; $AK = 0.11 \times 10^{-3}$; $CH = 0.01$; $BN = 4.0$; $BK = 15.4$; $P_a = 90$ mm Hg; $P_v = 34$ mm Hg. Lower part: Hypoxia case with a low arterial oxygen tension. Input parameters of the computer program: $AG = 8.17$; $AK = 0.25 \times 10^{-3}$; $CH = 0.01$; $BN = 5.22$; $BK = 2.97$; $P_a = 46.5$ mm Hg; $P_v = 28.0$ mm Hg.

[1] The CDC 3300 of the Computer Center, Johannes Gutenberg University, Mainz, was used for calculations.

[2] K. KUNZE, *Das Sauerstoffdruckfeld im normalen und pathologisch veränderten Muskel* (Springer Berlin, Heidelberg, New York 1969).

[3] D. W. LÜBBERS, in *Oxygen Transport in Blood and Tissue* (Thieme, Stuttgart 1968), p. 724.

[4] W. J. WHALEN and P. NAIR, Am. J. Physiol. *213*, 973 (1970).

[5] A. KROGH, J. Physiol., Lond. *52*, 409 (1918).

tion-profiles are neglected. g) Blood flow rate in diverse capillaries of the network is calculated according to Kirchhoff's Laws. In the case of con- and countercurrent system blood flow is assumed to be constant. h) Fick's first Law is valid at capillary tissue interface. Diffusion coefficient as well as solubility coefficient are assumed to be the same in tissues and capillaries. i) The reaction curve inside the capillaries is described by Hill's equation.

Mathematical description of the model. Oxygen exchange processes between capillaries and tissue are described by the following differential equations:

$$\text{Tissue } \frac{\partial^2 c}{\partial x^2} + \frac{\partial^2 c}{\partial y^2} - AG \frac{c}{c + CH} = 0$$

AG and CH are constants and defined as $AG = A\,l^2/\alpha\,P_a\,D$, $CH = P_K/P_a$.

$$\text{Capillary } \frac{\partial c}{\partial s} = \frac{AK}{f(c)} \left[\left(\frac{\partial c}{\partial n}\right)_+ + \left(\frac{\partial c}{\partial n}\right)_-\right]$$

where

$$f(c) = c^{m-1}/(1 + K\,P_a^m c^m)^2 .$$

AK is defined as:

$$AK = 100\,D\,\alpha\,P_a/1.34\,d\,v\,c_{Hb}\,m\,K\,P_a^m .$$

Results and discussion. The method of successive over-relaxation was used showing a better convergence than the method of successive displacements (METZGER[6,7]). To obtain stability of the iteration technique a relaxation parameter was found by trial and error (relaxation parameter: 1.25 to 1.82; accuracy: 0.005%; iteration meshwork: 1600 points per capillary square; iteration number: 400 steps).

Computer programs were based on partial differential equations of diffusion and chemical reaction in tissue as well as perfusion and chemical reaction in blood. Former calculations of other authors were performed for homogeneously perfused con- and countercurrent systems (THEWS[8], RENEAU, BRULEY, and KNISELY[9]). In this paper the inhomogeneously perfused capillary network model was used (Figure 1) and the results were compared with those obtained for con- and countercurrent systems.

[6] H. METZGER, Kybernetik *6*, 97 (1969).
[7] H. METZGER, Mathe. Biosci. *5*, 143 (1969).
[8] G. THEWS, Acta biotheor. *10*, 105 (1953).
[9] D. D. RENEAU, D. F. BRULEY and M. H. KNISELY, in *Chemical Engineering in Medicine and Biology* (Plenum Press, New York 1967).

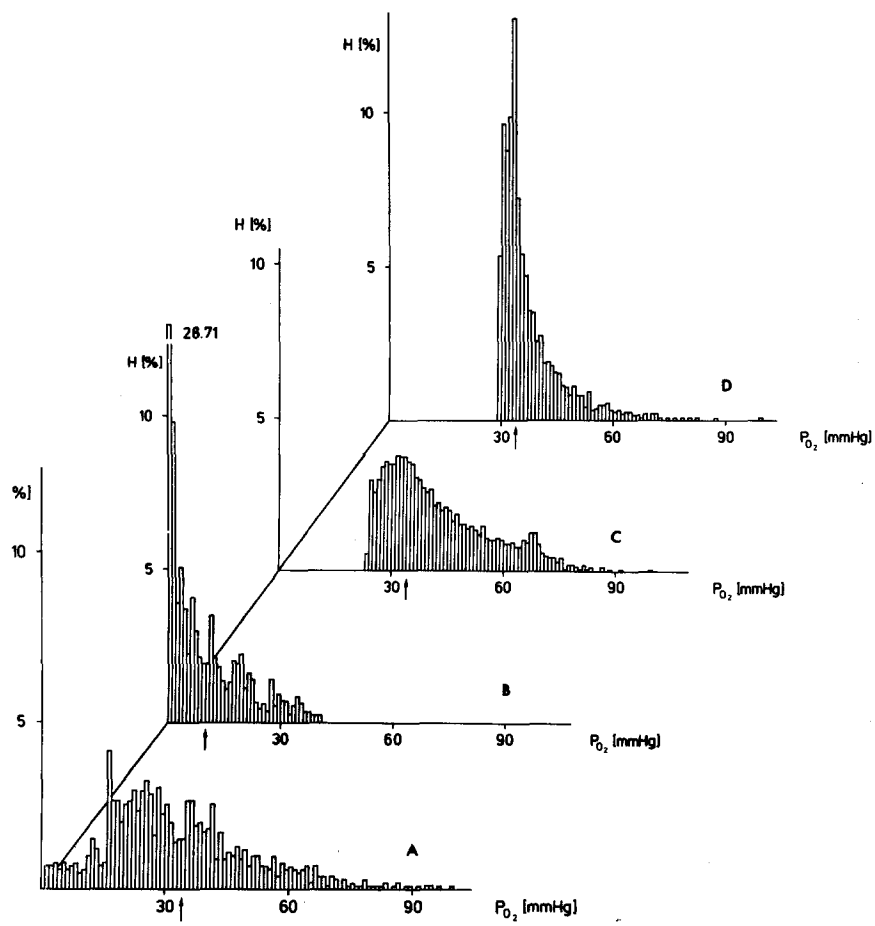

Fig. 3. Frequency distribution of oxygen tension values calculated for different capillary systems: A) network system (normoxia case). B) network system (hypoxia case). C) concurrent system (normoxia case). D) countercurrent system (normoxia case). Figure shows the broad oxygen tension spectrum of the network system (A). Under hypoxia a left shift of the spectrum occurs (B). The countercurrent system (D) has a typical histogram with a maximum in the range of venous oxygen tension. Arrows indicate venous oxygen tension. Input parameters of the computer program (normoxia): $AG = 3.18$; $AK = 0.59 \times 10^{-3}$; $CH = 0.01$; $BN = 2.83$; $BK = 39.2$; $P_a = 100$ mm Hg; $P_v = 34$ mm Hg. Input parameters for hypoxia, see Figure 2.

Oxygen tension distributions for normoxia and for hypoxia (P_a = 46.5 mm Hg) are demonstrated (Figure 2). During respiratory hypoxia the oxygen supply of some regions is not sufficient. From the oxygen tension distribution of the different capillary systems the histograms were derived. Oxygen tension histograms are illustrated for con- and countercurrent as well as capillary network systems (Figure 3). Furthermore, in the same figure an oxygen tension histogram for the hypoxia case is shown.

The figures demonstrate typical differences between oxygen tension histograms of the different capillary tissue models: the concurrent histogram is characterized by a homogeneous oxygen tension distribution with a oxygen tension spectrum between 23 mm Hg and arterial oxygen tension value of 100 mm Hg. Tissue points with values below the venous oxygen tension ar rarely seen. In the range between the venous and the arterial oxygen tension the frequency of oxygen tension values decreases more rapidly than in the concurrent histogram.

An extreme difference exists between homogeneously perfused con- or countercurrent systems and the inhomogeneously perfused capillary network. The capillary network has a broad spectrum ranging between zero mm Hg and the arterial oxygen tension of 100 mm Hg.

The analysis led to the conclusion that the frequently observed low oxygen tension values in brain tension (HEIDENREICH, ERDMANN, METZGER and THEWS[10] and METZGER[11]) might be caused by inhomogeneities in cerebral blood flow. A number of restrictions of this analysis should be kept in mind: homogeneity of oxygen consumption, isotropy of oxygen diffusion, equal solubility in all compartments, two-dimensional tissue area. Nevertheless, the present study of oxygen tension histograms help to better understand the experimental microelectrode results. This investigation demonstrates the tremondous influence of microcirculation and capillary architecture on oxygen tension distribution and histogram. A final proof of this conclusion will be obtained in a study on three-dimensional capillary arrangements.

Zusammenfassung. Mit Sauerstoff-Mikroelektroden werden die lokalen Werte des Sauerstoffpartialdruckes im Mikrobereich der Organe gemessen und graphisch als Häufigkeitsverteilungen (Histogramme) dargestellt. Theoretisch wird der Einfluss der Kapillaranordnung (Gleich-, Gegenstromsystem und Kapillarnetzwerk) auf die Häufigkeitsverteilung der P_{O_2} Werte untersucht. Die für zweidimensionale Modelle durchgeführte Analyse zeigt, dass Unterschiede in der Durchblutung, wie sie in den einzelnen Zweigen der Kapillarnetzwerke auftreten, einen starken Einfluss auf die Histogramme haben.

H. METZGER[12]

Department of Physiology, Johannes Gutenberg University, D-65 Mainz (West Germany), 13 December 1971.

Notations and constants: c = relative O_2 concentration or O_2 partial pressure. x, y = coordinates in tissue. n, s = capillary coordinates. l = capillary length = 60 µm. d = capillary side length = 6 µm. α = oxygen solubility coefficient = 0.025 ml/ml × Atm. diffusion coefficient = 2.10^{-5} cm²/sec. P_a = arterial oxygen tension = 100 mm Hg. P_v = venous oxygen tension = 34 mm Hg. P_K = critical oxygen tension = 1 mm Hg. m = Hill exponent = 2.83. K = Hill constant = 0.87×10^{-3}. c_{Hb} = hemoglobin concentration = 14 $g\%$. A = metabolic rate (grey matter) = ml/100 g × min. Δs = change of saturation of hemoglobin = 0.53. AG = 3.18. CH = 0.01. AK = 18 $AG \times K P_a^m m \times 100/\Delta s = 0.59 \times 10^{-4}$.

[10] J. HEIDENREICH, W. ERDMANN, H. METZGER and G. THEWS, Experientia *26*, 257 (1970).

[11] H. METZGER, *Verteilung des O_2-Partialdruckes im Mikrobereich des Gehirngewebes.* Polarographische Messung und Mathematische Analyse. Habilitationsschrift, Mainz 1971.

[12] Mailing address: Dr. Hermann Metzger, Rhodes Engineering Research Center, Clemson University, Clemson (South Carolina 29631, USA).

The Impairment of the Thermoregulatory 'Set-Point' of a Sheep in the Apparent Absence of Any Interference with the Pathways Between Temperature Sensors and Thermoregulatory Effectors

Core temperature of homeothermic mammals appears to be regulated at or near to an inherent but variable set-point, the neuronal nature of which remains obscure. VENDRIK[1], inspired by BAZETT[2], has suggested that this set-point function may depend on the activity/temperature characteristics of temperature-sensitive neurones in the preoptic area of the anterior hypothalamus (POAH), and some hypothalamic neurones have activity/temperature relations which are consistent with this proposal[3]. An alternative hypothesis, based on the existence of temperature-insensitive neurones in the POAH[4], is that these cells may exert an inhibitory influence on the temperature sensor to thermoregulatory effector pathways[5,6] thus creating threshold levels above which heat loss effectors, and below which heat production effectors, are activated. (For a more detailed discussion of these ideas see BLIGH[7]).

To study the effects on thermoregulation of interactions between changes in hypothalamic temperature (T_{hy}) and injections into a lateral cerebral ventricle of putative transmitter substances, a multiple thermode assembly was introduced into the POAH of sheep[8]. This inevitably involves some local brain damage but does not usually impair the capacity to thermoregulate. One sheep was unable, post-operatively, to regulate body temperature at the normal level for this species. The observations made on this animal indicate that the set-point mechanism may be distinct from the temperature-sensor to thermoregulatory-effector pathways.

The first indication of a post-operative disturbance was a high rectal temperature (T_{re}) of 41.5°C, which could have

[1] A. J. H. VENDRIK, Ned. J. Geneesk. *103*, 1 (1959).

[2] H. C. BAZETT, *Physiology of heat regulation* (Ed. L. H. NEWBURGH, Saunders: Philadelphia 1949).

[3] M. CABANAC, J. A. J. STOLWIJK and J. D. HARDY, J. appl. Physiol. *24*, 645 (1968).

[4] T. NAKAYAMA, H. T. HAMMEL, J. D. HARDY and J. S. EISENMAN, Am. J. Physiol. *204*, 1122 (1963).

[5] N. MURAKAMI, J. A. J. STOLWIJK and J. D. HARDY, Am. J. Physiol. *213*, 1015 (1967).

[6] J. D. HARDY, Columbia, Agric. exp. Sta. Special Report *103* (1969).

[7] J. BLIGH (1972), in *Essays on Temperature Regulation* (Eds. J. BLIGH and R. E. MOORE; Amsterdam, North Holland 1972).

[8] M. MASKREY and J. BLIGH, Int. J. Biochim. Biomet. *15*, 129 (1971).